

2.5-kV AlGaIn/GaN Schottky Barrier Diode on Silicon Substrate with Recessed-anode Structure

Ru Xu, Peng Chen*, Menghan Liu, Jing Zhou, Yunfei Yang, Yimeng Li, Cheng Ge, Haocheng Peng, Bin Liu, Zili Xie, Rong Zhang, Youdou Zheng

Key Laboratory of Advanced Photonic and Electronic Materials,
School of Electronic Science and Engineering, Nanjing University, Nanjing 210093, China

Abstract—In this letter, we demonstrate high-performance lateral AlGaIn/GaN Schottky barrier diodes (SBD) on Si substrate with a recessed-anode structure. The optimized rapid etch process provides results in improving etching quality with a 0.26-nm roughness of the anode recessed surface. By using the high work function metal Pt as the Schottky electrode, a low V_{on} of 0.71 V is obtained with a high uniformity of ± 0.023 V for 40 devices. Supported by the flat anode recess surface and related field plate design, the SBD device with the anode-cathode spacing of 15 μm show the $R_{on,sp}$ of 1.53 $\text{m}\Omega\cdot\text{cm}^2$ only, the breakdown voltage can reach 1592 V with a high power FOM (Figure-of-Merit) of 1656 MW/cm^2 . For the SBD device with the anode-cathode spacing of 30 μm , the breakdown voltage can be as high as 2521 V and the power FOM is 1244 MW/cm^2 .

Index Terms—AlGaIn/GaN, Lateral Schottky barrier diode, rapid etch process, breakdown voltage, power FOM

I. INTRODUCTION

GROUP III nitrides represented by GaN have a wide range of applications in optoelectronics and power electronics, which is considered to be one of the most important semiconductor materials after silicon. Owing to its superior material properties such as high electric breakdown field, high-electron saturation velocity, and high mobility in a readily available heterojunction 2-dimensional electron gas (2-DEG) channel, GaN has been widely used in high frequency and power electronic devices. Power electronic devices are one of the fundamental components in almost all electronic manufacturing industries, including the field of consumer electronics, wireless communications and industrial control. Among all device types, Schottky barrier diodes (SBD) are the essential components in power conversion systems, such as switching power supply, frequency converter, driver and other circuits.

Recently, high-performance GaN-based lateral SBD devices

This work is supported by National High-Tech R&D Project (2015AA033305), Jiangsu Provincial Key R&D Program (BK2015111), Collaborative Innovation Center of Solid State Lighting and Energy-saving Electronics, the Research Funds from NJU-Yangzhou Institute of Optoelectronics, the Research and Development Funds from State Grid Shandong Electric Power Company and Electric Power Research Institute. (*Corresponding authors: pchen@nju.edu.cn)

This work has ever been successfully submitted to the IEEE Electron Device Letters for possible publication in Sep. 2019, and the manuscript ID is EDL-2019-09-2015.

have received sufficient attention and many results have been reported, such as the SBDs with low V_{on} of 0.2~0.8 V, the breakdown voltages from 1 kV to 2.7 kV and a high-power figure-of-merit (FOM) of 2.65 GW/cm^2 [1]-[22]. According to the previous reports, in order to reduce the V_{on} , anode recess structure has been widely used for GaN lateral SBDs [4] [5]. Obviously, a good surface condition of the anode recess is the key factor to determine the final performance of the SBD. Most of the reported results adopted a complicated etch process to ensure controllable recess depth and minimize etch damage [1] [5] [6] [16] [21]-[23]. In order to realize an effective process and a good surface condition, a rapid anode recess etching method is proposed in this work, which can not only obtain a relatively precise recess depth, but also obtain a flat etching surface. Based on this etching technique and the special anode structure optimized in this work, high performance SBD devices can be demonstrated.

II. DEVICE FABRICATION

The sample was grown by metal organic chemical vapor deposition (MOCVD) on a 2-inch Si substrate. From the substrate, the device structure consists of a 5- μm high-resistance GaN buffer layer, a 200-nm i-GaN channel layer, a 1-nm AlN insertion layer, a 20-nm $\text{Al}_{0.25}\text{Ga}_{0.75}\text{N}$ barrier layer, a 2-nm carbon doped GaN cap layer and a 30-nm in-situ SiN_x passivation layer.

The SBD fabrication commenced with photolithography defining the SBD isolation area, and then putting the sample into buffered oxide etch (BOE) for 5 minutes to remove the SiN_x , finally a 400 nm isolation mesa was etched by inductively coupled plasma (ICP) by using Cl_2/BCl_3 .

In the second step, the electrode recess area was first defined by photolithography, and then the sample was put into BOE for 5 minutes to remove the SiN_x . The power of the RF/ICP was selected as 100W/300W during the ICP etching. The duration of the etching was 10 s, resulting in the etching depth about 25~27 nm measured by an atomic force microscope (AFM). Next, the sample was etched in a diluted KOH solution for 15 minutes in a water bath at 80 °C to remove all surface damages.

The last step was evaporation of electrodes, we used Ti/Al/Ni/Au (30/150/30/100 nm) as the ohmic electrode followed by rapidly annealing at 850 °C for 30 s in N_2 . The ohmic contact resistance (R_C) and sheet resistance (R_{SH}) were

0.67 $\Omega \cdot \text{mm}$ and 323 Ω/\square , respectively. Next, the anode metal Pt/Au (50/300 nm) was evaporated on the recessed area, which has a 2- μm overlap on the SiN_x passivation as the field plate.

Fig. 1.(a) shows the device structure. The SBDs feature a circular configuration with an effective width 220 μm . The anode-cathode spacing (L_{AC}) varies from 5 μm to 30 μm and the anode recess depth (d_R) varies from 12 nm to 33 nm. The internal electric field distribution of the SBD is shown in Fig. 1. (b). When there is no anode field plate (AFP), the electric field (EF) will concentrate at the edge of the anode at $V_{anode} = -300$ V. The result is that there is only one anode peak EF and the field intensity is very high at that spot. However, when an AFP is

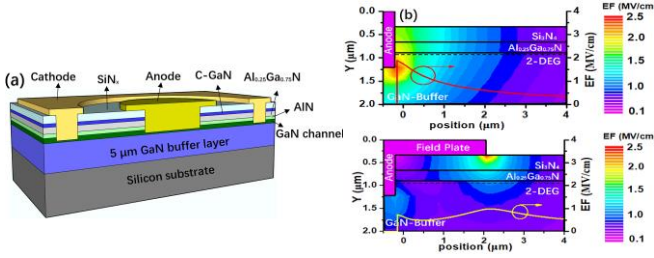


Fig. 1. (a) Cross-section view of the SBD device (b) internal electric field distribution of SBDs modulated by AFP

added to the anode, at $V_{anode} = -300$ V, the peak EF at the anode edge is reduced, the AFP dispersed the electric field, ultimately increasing the breakdown voltage of the SBD.

The SBD devices were analyzed by Silvaco-TCAD for the internal electric field distribution. The forward direct current (DC) measurements were carried out with a Keithley 4200 Semiconductor Parameter Analyzer and the reverse breakdown measurements were performed using an Agilent B1505A high-voltage semiconductor analyzer system.

III. RESULTS AND DISCUSSIONS

For the anode recess etching process, various etching methods have been reported, including high-temperature ICP etching, digital etching (dry and wet etching oxide layer circulation), two-step etching (ICP combined with digital etching), etc [24]-[26]. The advantages of these methods are that they can control the etching depth accurately and guarantee low etching damage. Although the controllability of the etching is increased, the efficiency of these methods is extremely low. For GaN E-mode HEMT, the accuracy of gate recess depth is very important. It requires a thin AlGaIn barrier for gate to deplete the 2-DEG. This means that the AlGaIn layer cannot be completely etched, which requires a high controllability of etching speed. However, for AlGaIn/GaN SBD, the accuracy of etching depth is not that important, as long as the anode is in direct contact with the GaN channel, and don't go deep into the GaN buffer. Reports and our experiment have shown that different etching depth of anode has no deep influence on the performance of the device [27], because it is the conduction between anode and cathode, the AlGaIn below the anode is not that important. This makes the range of anode recess depth larger. At this time, using the above method will no doubt increase the complexity of the device fabrication process.

However, most of the reported high-performance AlGaIn/GaN SBDs still use the above inefficient anode recess etching methods [1] [5] [6] [16] [21]-[23]. Thus, in order to develop an efficient etching method for recessed anode to improve the performance of the SBD, we did two different experiments. They were rapid etching method and slow etching method, the conditions were RF/ICP-100/300W and RF/ICP-10/100W, the etching time were 10s and 1min50s, respectively, the etching gas was a mixture of $\text{Cl}_2 / \text{BCl}_3$, the flow rate was 48 / 6 sccm, and the chamber pressure was 10 mtorr. Both of the etching

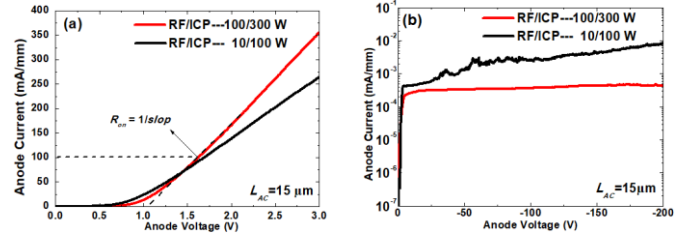


Fig. 2. I-V characteristics of two different anode-recess etching conditions (a) RF/ICP 100/300W (b) RF/ICP 10/100W (both after KOH solution wet etch)

depth are $\sim 25\text{nm}$, after etching, we put all the samples into a 0.1 mol/L KOH solution at 80 $^\circ\text{C}$ water bath for 15 min to remove the etch damage.

As shown in Fig. 2, two different etching methods show different results. For the rapid etching process, the V_{on} of the device is 0.71 V ($I_F=1$ mA/mm). Considering a 1.5- μm transfer length of ohmic contact and a 1.5- μm extension length of the Schottky contact, with the equation $R_{on, sp} = R_{on} \times (L_{AC} + 3)$, $R_{on, sp}$ is 1.53 $\text{m}\Omega \cdot \text{cm}^2$ ($I_F=100$ mA/mm). But for the slow etching process, the V_{on} of the device drops to 0.49 V, $R_{on, sp}$ rises to 2.48 $\text{m}\Omega \cdot \text{cm}^2$, and the leakage current also rises by more than

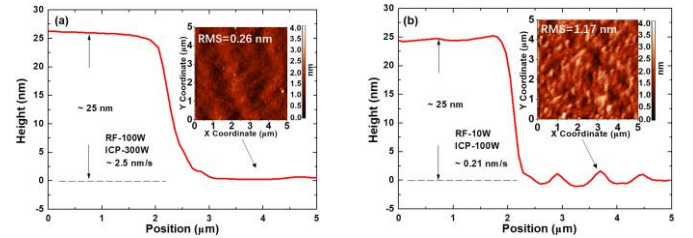


Fig. 3. AFM surface of two different anode-recess etching conditions (a) RF/ICP 100/300W (b) RF/ICP 10/100W (both after KOH solution wet etch)

an order of magnitude ($V_R=-200$ V), which means the slow-etching method has a larger damage to the surface and sidewall.

Although both of them have been modified under the same KOH condition, they show different results. In order to find out the cause of this phenomenon, we tested the surface of anode recess by AFM, as shown in Fig. 3, according to known reports, the slower the etching speed, the smoother the etching surface [5]. Although the etching speed has decreased, the damage caused by etching has not been removed, to remove the damage, we added a 0.1 mol/L hot KOH solution treatment after etching. Interestingly, after the treatment of KOH solution, the surface RMS of rapid-etched sample is only 0.26 nm, but the surface RMS of slow-etched sample is 1.17 nm, which shows that a

high-power etching with a short time can also obtain a flat surface.

Since hot KOH solution cannot fully remove the damage of slow etching, in order to further remove the etch damage, we put the slow-etched SBD into a rapid thermal annealing (RTA) for low-temperature annealing at a N_2 atmosphere, the temperature were 300 °C, 400 °C, 500 °C, respectively, and the annealing time was 5 min. The test results are shown in Fig. 4, we can find that the forward characteristics of slow-etched samples are significantly restored after RTA at low temperature compared with those of non-annealed samples, $R_{on,sp}$ recovers to the same level as the rapid-etched samples, which means the density of 2-DEG is also restored. However, for the reverse characteristics, we find that low-temperature post annealing could reduce the leakage current to a certain extent. As the annealing temperature rises from 300 °C to 500 °C, the leakage current of the SBD first decreases, and then rises to the level of the non-anneal sample. The effect of damage repair at 400 °C is the best, this is mainly because the N vacancy on the damaged surface is repaired by low-temperature annealing in

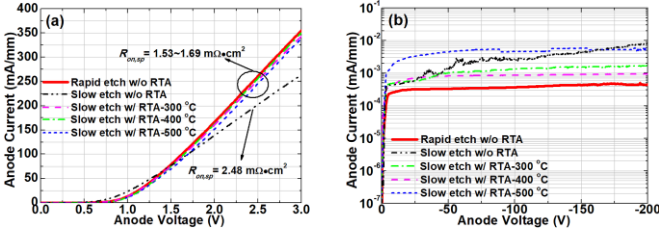


Fig. 4. I - V curves of different post annealing conditions (a) forward (b) reverse

the N_2 atmosphere, but the further rise of temperature can introduce new N vacancy on the GaN surface [28], so it is very important to choose the appropriate post annealing temperature. However, despite we did the post annealing experiments, the leakage current of the slow-etched sample is still larger than that of the rapid-etched sample.

Through the above experimental analysis, we selected RF/ICP-100/300W anode recess etching with a hot diluted KOH solution treatment as the condition of final device fabrication process.

As mentioned earlier in this paper, to explore the influence of different anode recess depth on the I - V characteristics of the SBD, four groups of devices with different anode recess depths were fabricated and analyzed, the recess depths of the four groups are non-recessed, 12 nm, 25 nm and 33 nm, respectively.

As shown in Fig.5, The non-recessed sample and the sample with the AlGaIn remained ($d_R=12$ nm) show a large V_{on} , both of which are more than 1V. When the etching depth reaches 25nm and 33nm, which means that the AlGaIn layer is completely etched, and go into the GaN channel layer. As can be seen from the figure, when the anode contacts with the GaN channel directly, the V_{on} reaches the minima. There is no difference in the V_{on} between the two samples, both of which are 0.71 V. We extracted the $R_{on,sp}$ of three SBDs in the same wafer with $d_R = 33$ nm, which ranges from 1.53 $m\Omega\cdot cm^2$ to 1.86 $m\Omega\cdot cm^2$ and the variation of which is within the acceptable range of error.

As for the leakage current, the largest leakage current is found in the non-recessed sample, due to the lack of post modification, the in-situ defects and surface states always exist, resulting in

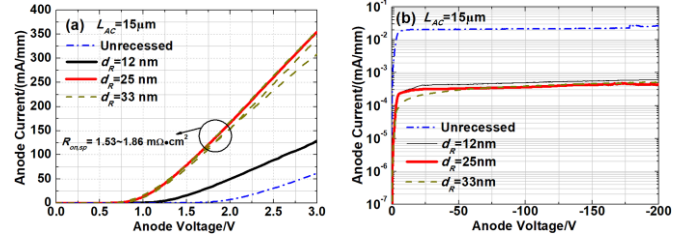


Fig. 5. Forward characteristics (a) and leakage current (b) for the devices with different anode recess depths d_R at room temperature.

the larger leakage current of the device. The leakage current of recessed and post-modified samples is kept in the order of 10^{-4} mA/mm, which is two orders of magnitude lower than the reported 2.07 kV GaN-on-Si sample [5].

Fig. 6. (a) shows the forward characteristics of 40 sets of $L_{AC}=15 \mu m$ SBDs with d_R of 25 nm on two different wafers. Fig. 6. (b) is the histogram statistics of V_{on} , the average V_{on} of the 40 SBDs is 0.71 V, while exhibiting a small standard deviation of

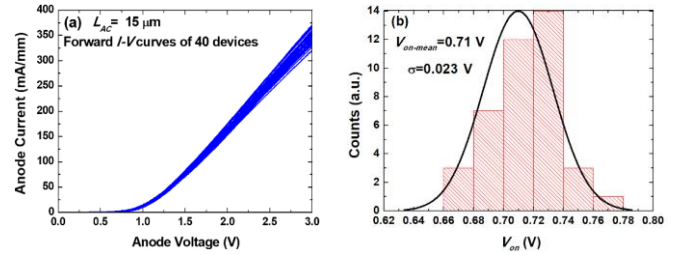


Fig. 6. I - V curves of 40 devices on two different wafers with $L_{AC}=15 \mu m$ (a) and distribution of V_{on} (b).

0.023 V. The $R_{on,sp}$ ranges from 1.44 $m\Omega\cdot cm^2$ to 1.79 $m\Omega\cdot cm^2$. It shows the extreme uniformity of the anode recess surface and demonstrates high repeatability of our rapid anode recess etch process.

Based on above results, considering both the forward and reverse characteristics, the SBD devices with anode recess depth of 25 nm have the best performance, which will be used in following study.

Fig.7 shows the forward I - V characteristics of the SBDs with

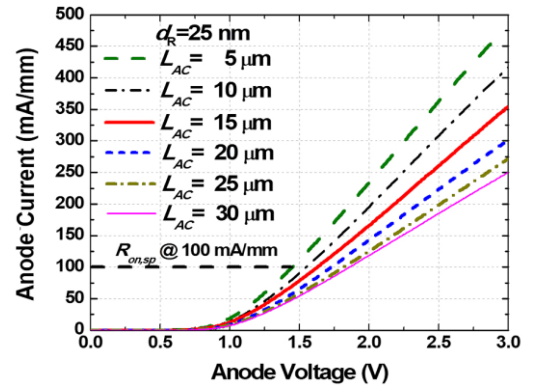


Fig. 7. Forward I - V characteristics of the SBDs with different L_{AC} of 5 μm , 10 μm , 15 μm , 20 μm , 25 μm and 30 μm .

different L_{AC} values (from 5 μm to 30 μm). The normalized forward operating current of the SBD with $L_{AC} = 5 \mu\text{m}$ and 15 μm can reach 237 mA/mm and 168 mA/mm at a forward bias of 3 V, respectively. Combined with a low leakage current below 0.0003 mA/mm, the current on/off ratio of these devices can be more than 10^8 within the range of -3 V to 3 V on the anode at room temperature. At the forward current density of 100 mA/mm, the $R_{on,sp}$ values of the SBDs with $L_{AC}=5 \mu\text{m}$ and $L_{AC}=15 \mu\text{m}$ are $0.45 \text{ m}\Omega \cdot \text{cm}^2$ and $1.53 \text{ m}\Omega \cdot \text{cm}^2$, respectively.

For Schottky forward characteristics, the I - V characteristic can be expressed by the theory of thermionic field emission (TFE) as:

$$I = I_s \times \left[\exp\left(\frac{qV - I \times R_s}{nkT}\right) - 1 \right] \quad (1)$$

Where R_s is the series resistance, T is the absolute temperature, k is the Boltzmann constant, n is the ideal factor, and I_s is the reverse saturation current. n and I_s can be obtained by the slope and intercept of the $\ln I$ - V curve, respectively. Meanwhile, the Schottky barrier height ϕ_b can be expressed as:

$$\phi_b = \left(\frac{kT}{q}\right) \times \ln\left(\frac{AA^*T^2}{I_s}\right) \quad (2)$$

Where A is the effective area of the device and A^* is the Richardson constant, after calculation, n and ϕ_b are 1.2 and 0.58 $\pm 0.04 \text{ eV}$, respectively.

The dynamic performance of the SBD is shown in Fig.8(a), the anode reverse pulse was set to 0~-800V with a step of -200V, pulse time was 30 ms, then, anode voltage was switched to positive values from 0~3 V with a step of 0.05 V to turn on the SBD. Fig. 8(b) shows the dynamic $R_{on,sp}$ of the SBDs with 15 μm L_{AC} under quiescent reverse bias from 0~-800 V with a stress time of 30 ms. there is only 0.12 V V_{on} shift when compared with the one without reverse stress under the same

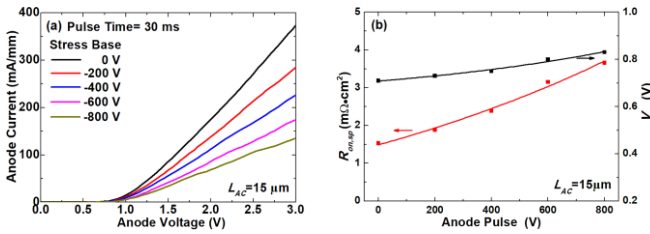


Fig. 8. (a) forward I - V characteristics of the GaN-on-Si SBDs with 30 ms time under various stress bases from -200 to -800 V at $L_{AC}=15 \mu\text{m}$. (b) Extracted dynamic $R_{on,sp}$ and V_{on} versus the reverse stress voltages

measurement setup. The dynamic $R_{on,sp}$ at -800 V reserve stress voltage is about 2.4 times the one without reverse pulse, which indicates that further optimization of passivation layer are needed.

Fig. 9.(a) shows the reverse I - V characteristics of the SBD at room temperature, with the L_{AC} changing from 5 μm to 30 μm . When a destructive-breakdown occurs, the voltage applied to the anode is defined as the breakdown voltage. The results show that the breakdown voltages of our SBD devices are 615 V ($L_{AC}=5 \mu\text{m}$), 1116 V ($L_{AC}=10 \mu\text{m}$), 1592 V ($L_{AC}=15 \mu\text{m}$), 1837 V ($L_{AC}=20 \mu\text{m}$), 2306 V ($L_{AC}=25 \mu\text{m}$) and 2521 V ($L_{AC}=30 \mu\text{m}$) respectively. We also tested five sets of the SBDs

with $L_{AC}=25 \mu\text{m}$, the breakdown voltages (BV) are all around 2300 V. Considering a 1.5- μm transfer length of ohmic contact and a 1.5- μm extension length of the Schottky contact, the power FOMs (FOMs = $BV^2/R_{on,sp}$) are 840, 1354, 1656, 1303,

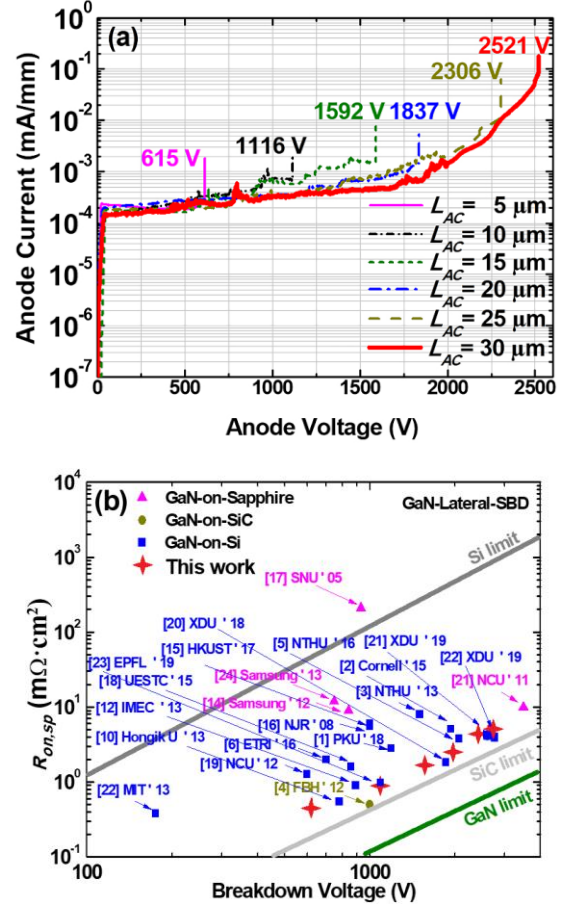


Fig. 9. (a) Reverse blocking characteristics of the SBDs as a function of L_{AC} from 5 μm to 30 μm and (b) benchmark plot of BV versus $R_{on,sp}$ for our lateral GaN-based SBDs.

1445 and 1244 MW/cm^2 for the SBDs with $L_{AC}= 5, 10, 15, 20, 25$ and $30 \mu\text{m}$ respectively. Our lateral GaN SBDs are benchmarked against some state-of-the-art lateral GaN SBDs (as shown in Fig. 9.(b)) [1]-[22].

IV. CONCLUSIONS

In this work, we developed the high-performance lateral SBDs by introducing a rapid anode recess etch technology to replace the conventional slow anode recess etch technology. The obtained anode recess surface has an RMS of only 0.26 nm and shows great improvement on the device performance. The repeatability test results show that the V_{on} is $0.71 \text{ V} \pm 0.03 \text{ V}$ among 40 SBD devices. When $L_{AC}=15 \mu\text{m}$, the breakdown voltage can reach 1592 V, $R_{on,sp}$ is $1.53 \text{ m}\Omega \cdot \text{cm}^2$, and the corresponding power FOM is as high as 1656 MW/cm^2 . By using this approach, the highest breakdown voltage is up to 2521 V, obtained in the SBDs with $L_{AC}=30 \mu\text{m}$, and the power FOM is 1244 MW/cm^2 correspondingly. Our results indicate that it is possible to achieve high-repeatability GaN SBDs with higher breakdown voltage on Si.

REFERENCES

- [1] J. N. Gao, Y. F. Jin, B. Xie, C. P. Wen, Y. L. Hao, B. Shen, and M. J. Wang, "Low on-resistance GaN Schottky barrier diode with high V_{ON} uniformity using LPCVD Si_3N_4 compatible self-terminated, low damage anode recess technology," *IEEE Electron Device Lett.*, vol. 39, no. 6, pp. 859–863, Jun. 2018, doi: 10.1109/LED.2018.2830998.
- [2] M. Zhu, B. Song, M. Qi, Z. Hu, K. Nomoto, X. Yan, Y. Cao, W. Johnson, E. Kohn, D. Jena, and H. G. Xing, "1.9-kV AlGaIn/GaN lateral Schottky barrier diodes on silicon," *IEEE Electron Device Lett.*, vol. 36, no. 4, pp. 375–377, Apr. 2015, doi: 10.1109/LED.2015.2404309.
- [3] Y. W. Lian, Y. S. Lin, J. M. Yang, C. H. Cheng, and S. S. H. Hsu, "AlGaIn/GaN Schottky barrier diodes on silicon substrates with selective Si diffusion for low onset voltage and high reverse blocking," *IEEE Electron Device Lett.*, vol. 34, no. 8, pp. 981–983, Aug. 2013, doi: 10.1109/LED.2013.2269475.
- [4] E. Bahat-Treidel, O. Hilt, R. Zhytnytska, A. Wentzel, C. Meliani, J. Würfl, and G. Tränkle, "Fast-switching GaN-based lateral power Schottky barrier diodes with low onset voltage and strong reverse blocking," *IEEE Electron Device Lett.*, vol. 33, no. 3, pp. 357–359, Mar. 2012, doi: 10.1109/LED.2011.2179281.
- [5] C. W. Tsou, K. P. Wei, Y. W. Lian, and S. S. H. Hsu, "2.07-kV AlGaIn/GaN Schottky barrier diodes on silicon with high Baliga's figure-of-merit," *IEEE Electron Device Lett.*, vol. 37, no. 1, pp. 70–73, Jan. 2016, doi: 10.1109/LED.2015.2499267.
- [6] H. S. Lee, D. Y. Jung, Y. Park, J. Na, H. G. Jang, H. S. Lee, C. H. Jun, J. Park, S. O. Ryu, S. C. Ko, and E. S. Nam, "0.34 V_T AlGaIn/GaN-on-Si large Schottky barrier diode with recessed dual anode metal," *IEEE Electron Device Lett.*, vol. 36, no. 11, pp. 1132–1134, Nov. 2015, doi: 10.1109/LED.2015.2475178.
- [7] J. G. Lee, B. R. Park, C. H. Cho, K. S. Seo, and H. Y. Cha, "Low turn-on voltage AlGaIn/GaN-on-Si rectifier with gated ohmic anode," *IEEE Electron Device Lett.*, vol. 34, no. 2, pp. 214–216, Feb. 2013, doi: 10.1109/LED.2012.2235403.
- [8] A. P. Zhang, J. W. Johnson, F. Ren, J. Han, A. Y. Polyakov, N. B. Smirnov, A. V. Govorkov, J. M. Redwing, K. P. Lee, and S. J. Pearton, "Lateral $Al_xGa_{1-x}N$ power rectifiers with 9.7 kV reverse breakdown voltage," *Appl. Phys. Lett.*, vol. 78, no. 6, pp. 823–825, Feb. 2001, doi: 10.1063/1.1346622.
- [9] S. Lenci, B. De Jaeger, L. Carbonell, J. Hu, G. Mannaert, D. Wellekens, S. You, B. Bakeroort, and S. Decoutere, "Au-free AlGaIn/GaN power diode on 8-in Si substrate with gated edge termination," *IEEE Electron Device Lett.*, vol. 34, no. 8, pp. 1035–1037, Aug. 2013, doi: 10.1109/LED.2013.2267933.
- [10] K. Park, Y. Park, S. Hwang, W. Jeon, and J. Lee, "1 kV AlGaIn/GaN power SBDs with reduced on resistances," in *Proc. IEEE 23th Int. Symp. Power Semiconductor Devices IC's*, May 2011, pp. 223–226, doi: 10.1109/ISPSD.2011.5890831.
- [11] J. C. Lei, J. Wei, G. F. Tang, Z. F. Zhang, Q. K. Qian, Z. Y. Zheng, M. Y. Hua, and K. J. Chen, "650-V double-channel lateral Schottky barrier diode with dual-recess gated anode," *IEEE Electron Device Lett.*, vol. 39, no. 2, pp. 260–263, Dec. 2017, doi: 10.1109/LED.2017.2783908.
- [12] A. Kamada, K. Matsubayashi, A. Nakagawa, Y. Terada, and T. Egawa, "High-voltage AlGaIn/GaN Schottky barrier diodes on Si substrate with low-temperature GaN cap layer for edge termination," in *Proc. IEEE 20th Int. Symp. Power Semiconductor Devices IC's*, May 2008, pp. 225–228, doi: 10.1109/ISPSD.2008.4538939.
- [13] S. C. Lee, M. W. Ha, J. C. Her, S. S. Kim, J. Y. Lim, K. S. Seo, and M. K. Han, "High Breakdown Voltage GaN Schottky Barrier Diode employing Floating Metal Rings on AlGaIn/GaN Hetero-junction," in *Proc. IEEE 17th Int. Symp. Power Semiconductor Devices & IC's*, May 23–26, 2005, pp. 247–250, doi: 10.1109/ISPSD.2005.1487997.
- [14] Q. Zhou, Y. Jin, Y. Shi, J. Mou, X. Bao, B. Chen, and B. Zhang, "High reverse blocking and low onset voltage AlGaIn/GaN-on-Si lateral power diode with MIS-gated hybrid anode," *IEEE Electron Device Lett.*, vol. 36, no. 7, pp. 660–662, Jul. 2015, doi: 10.1109/LED.2015.2432171.
- [15] Y. M. Hsin, T. Y. Ke, G. Y. Lee, J. I. Chyi, and H. C. Chiu, "A 600 V AlGaIn/GaN Schottky barrier diode on silicon substrate with fast reverse recovery time," *Phys. Status Solidi C*, vol. 9, no. 3–4, pp. 949–952, Mar. 2012, doi: 10.1002/pssc.201100343.
- [16] T. Zhang, J. C. Zhang, H. Zhou, T. S. Chen, K. Zhang, Z. Z. Hu, Z. K. Bian, K. Dang, Y. Wang, L. Zhang, J. Ning, P. J. Ma, and Y. Hao, "A 1.9-kV/2.61-m Ω -cm² Lateral GaN Schottky Barrier Diode on Silicon Substrate With Tungsten Anode and Low Turn-ON Voltage of 0.35 V," *IEEE Electron Device Lett.*, vol. 39, no. 10, pp. 1548–1551, Oct. 2018, doi: 10.1109/LED.2018.2864874.
- [17] G. Y. Lee, H. H. Liu, and J. I. Chyi, "High-Performance AlGaIn/GaN Schottky Diodes With an AlGaIn/AlN Buffer Layer," *IEEE Electron Device Lett.*, vol. 32, no. 11, pp. 1519–1521, Nov. 2011, doi: 10.1109/LED.2011.2164610.
- [18] E. Matioli, B. Lu, and T. Palacios, "Ultralow Leakage Current AlGaIn/GaN Schottky Diodes With 3-D Anode Structure," *IEEE Transactions on Electron Devices*, vol. 60, no. 10, pp. 3365–3370, Oct. 2013, doi: 10.1109/TED.2013.2279120.
- [19] J. Ma, G. Kampitsis, P. Xiang, K. Cheng, and E. Matioli, "Multi-Channel Tri-Gate GaN Power Schottky Diodes With Low ON-Resistance," *IEEE Electron Device Lett.*, vol. 40, no. 2, pp. 275–278, Feb. 2019, doi: 10.1109/LED.2018.2887199.
- [20] J.-H. Lee, C. Park, K.-S. Im, and J.-H. Lee, "AlGaIn/GaN-Based Lateral-Type Schottky Barrier Diode With Very Low Reverse Recovery Charge at High Temperature," *IEEE Transactions on Electron Devices*, vol. 60, no. 10, pp. 3032–3039, Oct. 2013, doi: 10.1109/TED.2013.2273271.
- [21] T. Zhang, J. C. Zhang, H. Zhou, Y. C. Zhang, T. S. Chen, K. Zhang, Y. Wang, K. Dang, Z. K. Bian, X. Duan, J. Ning, S. Zhao, and Y. Hao, "High-performance lateral GaN Schottky barrier diode on silicon substrate with low turn-on voltage of 0.31 V, high breakdown voltage of 2.65 kV and high-power figure-of-merit of 2.65 GW cm⁻²," *APPLIED PHYSICS EXPRESS*, vol. 12, no. 4, pp. 046502-1–046502-4, Mar. 2019, doi: 10.7567/1882-0786/ab0712.
- [22] T. Zhang, J. C. Zhang, H. Zhou, Y. Wang, T. S. Chen, K. Zhang, Y. C. Zhang, K. Dang, Z. K. Bian, J. F. Zhang, S. R. Xu, X. L. Duan, J. Ning, and Y. Hao, "A > 3 kV/2.94 m Ω -cm² and Low Leakage Current With Low Turn-On Voltage Lateral GaN Schottky Barrier Diode on Silicon Substrate With Anode Engineering Technique," *IEEE Electron Device Lett.*, vol. 40, no. 10, pp. 1583–1586, Oct. 2019, doi: 10.1109/LED.2019.2933314.
- [23] R. J. Shul, L. Zhang, A. G. Baca, C. G. Willison, J. Han, S. J. Pearton, and F. Ren, "Inductively coupled plasma-induced etch damage of GaN p-n junctions," *J. Vac. Sci. Technol. A*, vol. 18, no. 4, pp. 1139–1143, Jul. 2000, doi: 10.1116/1.582313.
- [24] S. Huang, Q. Jiang, K. Wei, G. Liu, J. Zhang, X. Wang, Y. Zheng, B. Sun, C. Zhao, H. Liu, Z. Jin, X. Liu, H. Wang, S. Liu, Y. Lu, C. Liu, S. Yang, Z. Tang, J. Zhang, Y. Hao, and K. J. Chen, "High-Temperature Low-Damage Gate Recess Technique and Ozone-Assisted ALD-grown Al₂O₃ Gate Dielectric for High-Performance Normally-Off GaN MIS-HEMTs," in *IEEE International Electron Devices Meeting*, Dec 15–17, 2014, pp. 14–442–445, doi: 10.1109/IEDM.2014.7047071.
- [25] Q. Zhou, B. W. Chen, Y. Jin, S. Huang, K. Wei, X. Y. Liu, X. Bao, J. Y. Mou, and Bo Zhang, "High-Performance Enhancement-Mode Al₂O₃/AlGaIn/GaN-on-Si MISFETs With 626 MW/cm² Figure of Merit," *IEEE Transactions on Electron Devices*, vol. 62, no. 3, pp. 776–781, Mar. 2015, doi: 10.1109/TED.2014.2385062.
- [26] S. H. Liu, S. Yang, Z. K. Tang, Q. M. Jiang, C. Liu, M. J. Wang, and K. J. Chen, "Al₂O₃/AlN/GaN MOS-Channel-HEMTs With an AlN Interfacial Layer," *IEEE Electron Device Lett.*, vol. 35, no. 7, pp. 723–725, Jul. 2014, doi: 10.1109/LED.2014.2322379.
- [27] Y. Park, J. Kim, W. Chang, H. Jang, J. Na, H. Lee, C. Jun, H. Cha, J. Mun, S. Ko, and E. Nam, "Low onset voltage of GaN on Si Schottky barrier diode using various recess depths," *IEEE Electronics Letters*, vol. 50, no. 16, pp. 1165–1167, Aug. 2014, doi: 10.1049/el.2014.1747.
- [28] D. W. Jenkins and J. D. Dow, "Electronic structures and doping of InN, In_xGa_{1-x}N, and In_xAl_{1-x}N," *Phys. Rev. B*, vol. 39, no. 5, pp. 3317–3329, Feb. 1989, doi: https://doi.org/10.1103/PhysRevB.39.3317.